

Fourier-Transform Rheology To Distinguish Polymer Solutions With Different Topologies

Thorsten Neidhöfer^{*}, Manfred Wilhelm^{**}

¹ Max-Planck-Institut für Polymerforschung, Ackermannweg 10, D-55128 Mainz, Germany
Fax: +49-6131-379100, E-mail: wilhelm@mpip-mainz.mpg.de;

^{*} Participant ^{**} To whom correspondence should be addressed.

Summary

The influence of the degree of branching on the non-linear relaxation behaviour of anionically synthesised polystyrene solutions was studied using FT-Rheology and compared with results obtained under oscillatory shear and step-shear conditions. FT-Rheology allowed to distinguish the different topologies where the other rheological measurements failed. Significant differences occurred under LAOS conditions as particularly reflected in the phase difference of the third harmonic, Φ_3 , which could be related to shear thinning and shear thickening behaviour. Currently, this work is extended towards long-chain branching in polyolefines.

Keywords: FT-Rheology; LAOS; viscoelastic properties; branched polymers; polystyrene

I. Introduction

Fourier transformation (FT) in combination with LAOS experiments (FT-Rheology) was applied in several publications as a promising technique to describe non-linear phenomena of polymeric materials^[1,2,3,4,5,6]. Technical and especially computing power limitations prevented further progress at that time. The groups of Prof. Dealy and Prof. Giacomin used this technique within sliding-plate rheometer studies^[7,8,9,10]. In difference to former work, the group of Dr. Wilhelm has developed and used an extremely sensitive detection system in combination with a specific FT algorithm on commonly available rotational rheometers^[11,12,13,14]. Several modifications led to an overall improvement of a factor 100 - 1000 in signal-to-noise ratio compared to former work^[15,16]. These differences allow to detect and to quantify much smaller differences.

The fundamental theoretical aspects of high sensitivity FT-Rheology can be found in recent publications^[11,13,17]. Under large amplitude oscillatory shear conditions (LAOS) with excitation frequency ω_1 , the non-linear stress response of any material is still periodic but not a single sinusoidal any more. The FT-Rheology technique uses the Fourier transformation of the stress (torque) signal as a function of time to resolve different frequency components. Only the fundamental at $\omega_1/2\pi$ and higher-order odd harmonics appear within the resulting frequency spectrum described by a magnitude $I(n\omega_1)$ and a related phase $\phi(n\omega_1)$ ($n = 1, 3, 5, \dots$)^[13,17]. A possible way to quantify the degree of non-linearity is the ratio $I_{n/1} \equiv I(n\omega_1)/I(\omega_1)$ of the magnitude for the n^{th} harmonic $I_n \equiv I(n\omega_1)$ with respect to the fundamental frequency $I_1 \equiv I(\omega_1)$. Using $I_{n/1}$ instead of simply I_n results in a significantly increased reproducibility because experimental variations i.e. in the sample preparation are compensated due to this normalisation procedure^[13,15].

A descriptive function was recently presented by Wilhelm^[13] for $I_{n/1}$ as a function of γ_0 for constant ω_1 which originated from the idea that for weakly non-linear deformations $I_1 \propto \gamma^1$ and $I_3 \propto \gamma^3$, thus $I_{3/1} \propto \gamma^2$ ^[18,19].

$$I_{3/1}(\gamma_0) = A \cdot \left(1 - \frac{1}{1 + (B\gamma_0)^C} \right). \quad (1)$$

Equation 1 has three adjustable parameters. Parameter A is the maximum intensity of $I_{3/1}$, the plateau for large shear amplitudes (typically: $A = 0.2 \pm 0.1$), C is the power law dependence for small strain amplitudes (Helfand and Pearson^[18] and Pearson and Rocheford^[19] predicted: $C = 2$) and B is a critical inverse strain amplitude close to the pivot point of Equation 1. If $\gamma_0 = 1/B$ the relative intensity of the third harmonic, $I_{3/1}(\gamma_0)$, equals $A/2$.

Prior to the work of the group of Dr. Wilhelm, Giacomin and Dealy^[7] presented a way to analyse the relative phase of the higher harmonic response where they related the spectral components of the stress response, ϕ_n , to the phase of the strain wave, ϕ_γ . Within this notation, the phase difference of the n^{th} harmonic is defined as

$$\Delta\phi_n \equiv \phi_n - n \cdot \phi_\gamma. \quad (2)$$

In contrast, Neidhöfer and coworkers ^[17] recently introduced a route to analyse the relative phase of the higher harmonic response as a potential characterisation parameter for the measured stress data versus time in the non-linear regime. In this new notation, the harmonic phases of the stress response, ϕ_n , are correlated to the phase of the fundamental, ϕ_1 , and are quantified by the relative phase difference ^[17]

$$\Phi_n \equiv \phi_n - n \cdot \phi_1 . \quad (3)$$

In contrast to Equation 2, the phase difference as defined by Equation 3 quantifies thinning (softening) respectively thickening (hardening) behaviour independently of the phase of the exciting strain wave, thus independent of the information about viscosity and elasticity which is already expressed by $\tan \delta$. For clarification of the pros and cons of both notations, the nonlinear stress response of a nonlinear spring element and a nonlinear dashpot element are analysed separately. For a periodic excitation in the linear regime, the stress response σ of a spring linearly depends on the deformation γ where the shear modulus G is the proportionality constant. Thus, the stress wave instantaneously follows the strain wave. If we now assume a nonlinear stress response solely of a spring, the shear modulus becomes a function of γ , not $\dot{\gamma}$, and can be Taylor expanded with respect to γ :

$$G(\gamma) = G_0 + G_2 \cdot \gamma^2 + \dots . \quad (4)$$

Here, we consider only the even higher-order terms due to the symmetry of the underlying shear properties. For simplicity and under the assumption of a weak nonlinear response we only consider the first nonlinear term. With $\sigma = G \cdot \gamma_0 \cdot \sin(\omega_1 t)$ and Equation 4, the stress wave results to

$$\sigma(t) = [G_0 + G_2 \cdot \sin^2(\omega_1 t)] \cdot \gamma_0 \sin(\omega_1 t) . \quad (5)$$

In case a strain hardening behaviour is observed, $G_2 > 0$, while a strain softening behaviour is reflected by $G_2 < 0$. Two substantial criteria can be established for the resulting stress waves of these two cases. Firstly, the two stress waves are in phase with the strain wave as indicated by $\delta = 0^\circ$. Secondly, the two waves reflecting softening and hardening behaviour, respectively, obey different shapes. In the softening case, a more rectangular shape will be observed while the hardening behaviour will be expressed by a more triangular shape. Analysis of these stress waves provides $\Phi_3 = 180^\circ$ and $\Delta_3 = 180^\circ$ for the softening behaviour and $\Phi_3 = 0^\circ$ and $\Delta_3 = 0^\circ$ for the hardening case (Table 1). Therefore, both notations (Equation 2 and Equation 3) lead to the same numerical values in case of a nonlinear spring.

For a periodic excitation in the linear regime, the stress response σ of a nonlinear dashpot linearly depends on the shear rate $\dot{\gamma}$ where the dynamic viscosity η is the proportionality constant. In the nonlinear regime, the viscosity becomes a function of the shear rate and can be approximated via a polynomial with respect to the shear rate:

$$\eta(\dot{\gamma}) = \eta_0 + \eta_2 \cdot \dot{\gamma}^2 + \dots \quad (6)$$

As for the spring, we only consider the first nonlinear term here. With $\sigma = \eta \dot{\gamma} = \eta \gamma_0 \omega_1 \cos(\omega_1 t)$ and Equation 6, the stress wave results to

$$\sigma(t) = [\eta_0 + \eta_2 \cdot (\gamma_0 \omega_1 \cos(\omega_1 t))^2] \cdot \gamma_0 \omega_1 \cos(\omega_1 t) . \quad (7)$$

A shear thickening behaviour is observed if $\eta_2 > 0$ while shear thinning is expressed by $\eta_2 < 0$. Both stress waves are 90° out of phase to the strain wave. Shear thinning will be reflected by a more pronounced rectangular shape while a more pronounced triangular shape will be found in case the response is shear thickening. From analysis we obtain $\Phi_3 = 180^\circ$ and $\Delta_3 = 270^\circ$ for the softening behaviour and $\Phi_3 = 0^\circ$ and $\Delta_3 = 90^\circ$ for the hardening case. The different analytical results for $I_{3/1}$, Φ_3 , and Δ_3 for the selected, simple phenomenological models and, in addition, constitutive and molecular models are compared in Table 1.

If we compare the resulting phase differences of a spring and a dashpot under nonlinear conditions, we find the thinning (softening) behaviour always be reflected by $\Phi_3 = 180^\circ$ and a thickening (hardening) behaviour always by $\Phi_3 = 0^\circ$ in our notation. At the same time, the linear viscoelasticity can be interpreted based on $\tan \delta$. The primary advantage of our notation therefore is that information can easier be extracted from data due to this separation.

The analysis of the relative phase of higher-order contributions is in analogy to the Lissajous figures ^[7] which are obtained by plotting the shear stress versus the shear strain. However, this new analysis results in more precise and quantitative data since it is even difficult to experimentally detect and quantify deviations from the linear mechanical response within a Lissajous figure especially at lower

nonlinearities, e.g. $I_{3/1} < 0.03$. Furthermore, Lissajous figures cannot unravel the contribution of intensity and phase of the higher harmonics.

In this work, for the first time FT-Rheology is applied for mechanical characterisation of linear and star-branched polymer solutions and compared to common linear and nonlinear mechanical characterisation methods. Of particular importance is to elaborate the effect of topology towards the linear and non-linear mechanical response as seen by several mechanical characterisation techniques.

II. Experimental Part

A. Setup

Data were obtained using a Rheometric Scientific ARES rheometer equipped with a 2KFRTN1 torque transducer. The raw time data from the force transducer was externally digitized using a 16-bit analog-to-digital converter (ADC) card (PCI-MIO-16XE; National Instruments, Austin, USA). This allowed the measurement and averaging ("oversampling") of the shear strain and the shear torque on the fly^[16] and extended the minimum detectable stress by a factor of roughly 5 and the signal to noise ratio (S/N) within FT spectra by a factor of 100 - 1000. LabVIEW 5.1 routines (National Instruments) were used to acquire raw time data and to apply Fourier transformation (FT) analysis. All polymer solutions were measured using a cone-plate geometry with a diameter of 25 mm and 0.02 rad cone angle.

B. Samples

Four different polystyrene solutions in iso-dioctyl phthalate (DOP) were studied: two linear PS solutions (PS250_41, PS400_30) and two star PS solutions (PS3Star_47, PS4Star_47) (see Table 2). Using inert-atmosphere techniques^[20,21,22], the linear polymer solutions were anionically synthesized polystyrenes (PS) of molecular weight above the entanglement molecular weight of $M_e = 13.3$ kg/mole^[23]. The star polymers were synthesised by reacting anionically polymerised living PS chains with the appropriate chlorosilane using high-vacuum techniques^[24]. For the three-arm star polymer this was trichloromethylsilane and for the four-arm star polymer 1,2-bis-(dichloromethylsilyl)-ethane. All polymers were dissolved in DOP according to the relation^[25]:

$$Z^{\text{sol}}/Z = c^{4/3} \quad (3)$$

where Z^{sol} and Z refer to the number of entanglements in solution and melt, respectively, and c to the polymer weight fraction in the solution. Dichloromethane was used as co-solvent to prepare the solutions and was afterwards removed gradually at room temperature under vacuum. For these polymer solutions, the Flory θ -temperature is $T_\theta = 295$ K^[26] and the entanglement number in average $Z^{\text{sol}} \cong 6.1$.

C. LAOS measurements

Within the range of applied strain amplitudes, all measurements were carried out under stable steady-state periodic conditions. For each experiment, 20 cycles were recorded to quantify the higher harmonics in terms of magnitude, $I_{n/1}$, and phase, Φ_n . The concept of the Deborah number, $De = \omega/\omega_0$, was used in order to study the frequency dependence especially of the nonlinear viscoelastic behaviour. Neidhöfer and coworkers^[17] established for linear polystyrene solutions that the non-linear response scales with the Deborah number rather than simply the excitation frequency, $\omega_1/2\pi$. The polymer samples were measured at excitation frequencies where the Deborah numbers range between $De \cong 0.06$ and $De \cong 60$, therefore covering three decades in which the response changes from purely viscous ($De \ll 1$) to almost elastic ($De \gg 1$).

III. Results And Discussions

To characterise the four different PS solutions in the linear viscoelastic regime master curves for the frequency dependent G' and G'' were shifted using the time-temperature superposition principle (Figure 1). They are referenced to the cross-over point of G' and G'' located between the terminal and the entanglement zone which we assume to reflect the longest relaxation time, τ_d , of these polymer solutions. The solutions show comparable polydispersities and are fairly monodisperse (see Table 2). It is due to the low amount of entanglements that the samples cannot be distinguished in the linear regime within experimental error. Differences start to appear in G'' in the higher frequency range above $\omega \cdot a_T \cdot \tau_d \approx 10$. These are due to slight differences in Z^{sol} which influence the length of the entanglement plateau. We were not able to carry out experiments at frequencies higher than those reported here since at low temperatures required for such measurements, phase separation occurred, reflecting the reduced solvent quality of DOP.

In addition to oscillatory measurements, the different polymer solutions were exposed to linear and non-linear single step-strains and the stress relaxation was measured as a function of time. The relaxation modulus $G(t)$ as a function of time is given in Figure 2A for PS250_41 at $T = 321.7$ K. $G(t)$ is nearly factorable into a time- and a strain-dependent term: $G(\gamma, t) = G(t) \cdot h(\gamma)$ [27,28,29,30]. On a molecular level, the nonfactorable relaxation that occurs in Figure 2A at times shorter than $\tau_r \approx 0.15$ s is caused by incomplete retraction [31,32,33,34]. After a step-strain the tube and the chain within are stretched affinely and the molecule relaxes this stretch by retraction along its contour back to its equilibrium value. Consequently, no new topological constraints are introduced. The characteristic relaxation time τ_r is roughly equal to the Rouse relaxation time τ_R . At times longer than τ_r retraction is completed. The damping functions for PS3Star_47 and PS250_41 are given in Figure 2B along with a theoretical predictions by Doi and Edwards [35]. The strain softening detected in $h(\gamma)$ is attributed to the retraction process. Within the experimental error range the $h(\gamma)$ data for the linear solutions (represented by PS250_41) and the star solutions (represented by PS3Star_47) agree with each other and, in addition, the data follow the Doi-Edwards prediction. This is in agreement with observations for monodisperse, entangled polymer melts and solutions ($Z \cong 5 - 50$) [27,36,37,38]. The strong reduction of the stress on large strains is explained by the rapid retraction of chains within strained (and therefore extended) tubes. Such retraction is not hindered in the case of star-shaped polymers because it depends on the curvilinear mobility of the free end. In star polymers, every chain segment is topologically connected to a chain end, and so it may retract as rapidly within its tube as a linear chain.

For the shear stress response under LAOS conditions as obtained within the FT-Rheology experiment Neidhöfer and coworkers [17] assumed a time-shear amplitude separation in the frequency space which they presumed to be reflected by the relative intensity of the third harmonic $I_{3/1}(\gamma_0)$. Here, it was of interest whether or not topology influences this time-shear amplitude separation in the frequency space under LAOS conditions. Therefore, $I_{3/1}(\gamma_0)$ was measured as a function of strain amplitude, γ_0 , at various Deborah numbers below and above $De = 1$ (Figure 3A).

The strain amplitude was increased until $I_{3/1}(\gamma_0) \approx 0.05$. For higher nonlinearities secondary flows or edge effects are expected to play an increasing role and the reproducibility of the measurements and the achievement of a dynamic steady state regime can no longer be ensured. Within this range of strain amplitudes the measurements at $De \approx 1$ reveal the highest nonlinear response, whereas for both higher and lower Deborah numbers $I_{3/1}(\gamma_0)$ is lower at comparable γ_0 . In extension to the results presented by Neidhöfer and coworkers [17], a scaling dependence of $I_{3/1}$ onto the strain amplitude was found for all curves even for $De > 1$, where the sample response is preferentially elastic. Despite this agreement, the results indicate that the constant slope of $C = 1.46$ found for linear polymer solutions in the flow regime [17] seems to change when the sample response is more elastic.

For quantification, the different curves given in Figure 3A were fitted using Equation 1 [13,17]. The obtained C parameters are plotted in Figure 3B as a function of the Deborah number, De , for the four different polystyrene solutions under investigation. Indeed, the C parameter is found to be independent of De if $De < 1$, and becomes a function of De if $De > 1$. In particular, C decreases therefore reflecting less strain softening. The latter observation reveals that the time-shear amplitude separation under LAOS conditions, as expressed by Equation 1, is not universal but clearly influenced by nonlinear elastic terms. Thus, even an empirical functionality between $I_{3/1}$ and γ_0 similar to that detected under step-shear conditions cannot be formulated here. The results on linear PS solutions presented by Neidhöfer and coworkers [17] gave rise to the idea that beside the time-shear amplitude separation a dynamic orientation process, thus a memory-related contribution, is expressed in the strain dependence of $I_{3/1}$. In view of this idea, one might argue about the presence of a universal time-shear amplitude separability in the frequency space and an influence of elasticity towards such an orientation process. The question whether this hypothesis is true or not can only be solved by taking sophisticated molecular models into account. Another remarkable finding is that especially for $De < 1$ the C parameters for the star solutions appear to be slightly higher compared to those for the linear solutions although the differences are weak. It turns out that the time-shear amplitude separation as detected under LAOS conditions and quantified by the ratio $I_{3/1}$ therefore is rather insensitive towards the topology of the investigated samples. Although the maximum shear rates within one cycle in general are much lower under LAOS conditions, the corresponding time-shear amplitude separability might be related to that found under single-step shear conditions.

To be able to compare the nonlinear response of the different polymer solutions under LAOS conditions in a proper way, $I_{3/1}$ is plotted in Figure 4 for both the linear and the star solutions as a function of De at a strain amplitude $\gamma_0 = 2$. The intensity ratio reaches its highest values in the range of the longest relaxation time of the polymer solutions; $I_{3/1} \cong 0.045$ for all different samples. No significant differences due to the polymers topology are detected within the range of Deborah numbers except at

higher Deborah numbers. These differences originate from slightly lower numbers of entanglements, Z^{sol} , for the star solutions compared to the linear solutions (see also Figure 1). The relation between the longest relaxation time, τ_d , and the Rouse relaxation time, τ_R , as obtained from molecular models, is given as ^[39,40].

$$\tau_d/\tau_R = 3 \cdot Z. \quad (8)$$

For the polymer solutions measured within this publication the Rouse relaxation is expected to appear at $De \geq 18.3$. It is remarkable that for $De > 20$ where the relaxation times are smaller than τ_R , a plateau seems to appear which is lower in intensity by a factor of 4 - 5 compared to the maximum intensity at $De \cong 1$ for $\gamma_0 = 2$. This observation might be better understood by interpreting the results in view of phenomenological models. Therefore, the Maxwell model is extended in a simple way via a nonlinear responding dashpot with $\eta = \eta_0 + \eta_1 \cdot \dot{\gamma}^2$ - representing the viscous contribution - and a linear responding spring with $G = \text{const.}$ - representing the elastic contribution - arranged in series. For slow motions, the relaxation is dominated by the linear viscous response (η_0) of the dissipative element, the dashpot. Under fast excitation motion, the relaxation behaviour is controlled by the linear elastic response (G) of the spring. In between, the relaxation is influenced by the non-linear response (η_1) of the dashpot. For polymers, this relaxation is shear thinning (therefore η_1 is negative) which results in a decrease of the viscosity and an increase of $I_{3/1}$.

A new and most promising parameter in FT-Rheology to distinguish topologies is the phase difference of the third harmonic, Φ_3 ^[17]. To analyse the phase information in an appropriate manner, Φ_3 for two linear and two star solutions is plotted as a function of De at a strain amplitude of $\gamma_0 = 2$ (Figure 5). Within the range of experimentally accessible Deborah numbers, values lower than 180° are obtained corresponding to a shift of the maxima / minima to the left side within the torque as a function of time (see [17] for details). For both low strain amplitudes and low Deborah numbers, where the sample response is dominantly viscous, Φ_3 is close to 180° . At $De \cong 1$, thus in the range of the longest relaxation processes of the entangled polymer chain, a local minimum is reached as characterised by $\Phi_3 = 100^\circ - 105^\circ$ for the linear solutions and $\Phi_3 = 90^\circ$ for the star solutions. At $De = 10-20$ a local maximum occurs quantified by $\Phi_3 \cong 120^\circ$ for the linear solutions and $\Phi_3 \cong 105^\circ - 110^\circ$ for the star solutions. According to Equation 8, the Rouse relaxation time, τ_R , should appear at $De = 18.3$ for $Z^{\text{sol}} \cong 6.1$ and might be correlated to this maximum. Below $De = 50$ for the linear solutions and below $De = 20$ for the star solutions, the samples response reflects a shear thinning behaviour expressed by Φ_3 values well above 90° . This corresponds to relaxation times $\tau \geq \tau_R$ which can be addressed to the orientation relaxation processes ^[40]. For higher De , a stronger decrease is detected. Beyond $De > 50$ for the linear solutions and beyond $De > 20$ for the star solutions, Φ_3 drops below 90° . According to our notation, the sample behaviour can then be interpreted as primarily shear thickening for these higher Deborah numbers. To get a heuristic understanding for this shear thickening behaviour, for shear faster than the inverse Rouse relaxation, mainly a stretch relaxation mechanism, has to be considered ^[41,42,43,44,45]. According to that mechanism, a stretch of the polymer chain can be interpreted as a thickening process which is in agreement with the observed behaviour as reflected by Φ_3 .

The $\Phi_3(De)$ dependence for the linear solutions coincide within the experimental error just as those for the star solutions, independent of the number of arms of the star molecule. The local maximum for the star solutions is shifted to lower Deborah numbers compared to the linear solutions which can be addressed to slightly lower numbers of entanglements. Beside these agreements between linear and star solutions significant differences arise. They are especially pronounced in the areas of both the local minimum and the local maximum where the values of Φ_3 are roughly $15^\circ - 20^\circ$ lower for PS4Star_47 than for PS250_41. At comparable Deborah numbers and strain amplitudes the star solutions therefore respond less thinning than the linear chain solutions under the applied conditions.

The observed differences in Φ_3 between star and linear solutions are significantly larger than the experimental error due to reproducibility or variations within one measurement. Consequently, it is possible to distinguish star shaped and linear topologies based on Φ_3 . This was neither possible in the linear oscillatory regime (see Figure 1) nor in the nonlinear regime under step-shear conditions (see Figure 2). The less-thinning effect found for the star solutions compared to the linear ones might be explained in view of the different relaxation processes presumed for stars due to the introduced branch point (see e.g. [40]). According to these theories, a star molecule cannot reptate and its arms relax the stress by retracting along their contour. We assume, that this retracting and pulling along the contour primarily accounts for the less-thinning effect. The basic idea behind this assumption is that under comparable conditions the segments in a star chain might be stretched or compressed more than in linear chains. Consequently, a hindered convective constraint release for the stars would explain the results on a qualitative level. Nevertheless, constitutive models like e.g. the pom-pom model ^[46] that

take molecular parameters into account have to be applied in order to find an appropriate explanation for the observed differences between linear and star solutions.

The phase difference quantifies the shift of the maxima / minima to the left or right side within the time response and is found to be very sensitive towards the topology of the analysed sample. The results found for the polymer solutions give rise to the idea that a higher degree of branching, such as in H-shaped polymers, comb structures, or long-chain branched polyethylene, could be distinguished by Φ_3 .

IV. Conclusions

We investigated the influence of the degree of branching on the linear and non-linear relaxation behaviour of polymeric materials by employing in particular FT-Rheology and other rheological techniques to variously branched polymer melts and solutions. Linear and star-shaped polystyrene solutions behaved similar in the linear viscoelastic regime and under non-linear step-shear conditions whereas significant differences occurred under LAOS conditions. The most pronounced difference between the samples could be achieved via the analysis of the phase of the third harmonic Φ_3 which is related to shear thinning and shear thickening behaviour under oscillatory shear. In particular, the response of the star-shaped solutions under LAOS conditions was less thinning than that of the linear solutions. In accordance with molecular theories, shear thinning and shear thickening behaviour could be attributed to orientational and stretch relaxation, respectively, as different time scales were interrogated by FT-Rheology. Shear thinning and shear thickening under oscillatory conditions were clearly distinguishable based on the phase Φ_3 .

Acknowledgement

This work was supported by the Max-Planck Gesellschaft. The authors are very grateful to Prof. N. Hadjichristidis, Dr. S. Sioula, and Dr. A. Avgeropoulos for assisting to synthesis the star-branched polystyrene samples. The authors thank Prof. H.W. Spiess and Prof. T. Pakula for scientific support and stimulating discussions.

Tables & Figures

Table 1:

model	$I_{3/1}$	Φ_3	$\Delta_3^{(*)}$
Maxwell	0	-	-
nonlinear spring, softening	$\neq 0, \infty \gamma_0^2$	180°	180°
nonlinear spring, hardening	$\neq 0, \infty \gamma_0^2$	0° (360°)	0° (360°)
nonlinear dashpot, softening	$\neq 0, \infty \gamma_0^2$	180°	270°
nonlinear dashpot, hardening	$\neq 0, \infty \gamma_0^2$	0° (360°)	90°
nonlinear Maxwell constitutive and molecular models (e.g. Pom-Pom)	no analytical solution via simulation		

(*) according to Giacomin and Dealy^[7]

Table 2:

sample	M_w [kg/mole]	M_w / M_n	c [wt]	M_e^{sol} [kg/mole]	Z^{sol}
PS250_41	262.8	1.08	0.41	67.5	6.1
PS400_30	401.9	1.10	0.30	103.0	6.1
PS3Star_47	303.0	1.07	0.47	52.0	6.1
PS4Star_47	408.8	1.07	0.47	52.0	6.1

Figure 1:

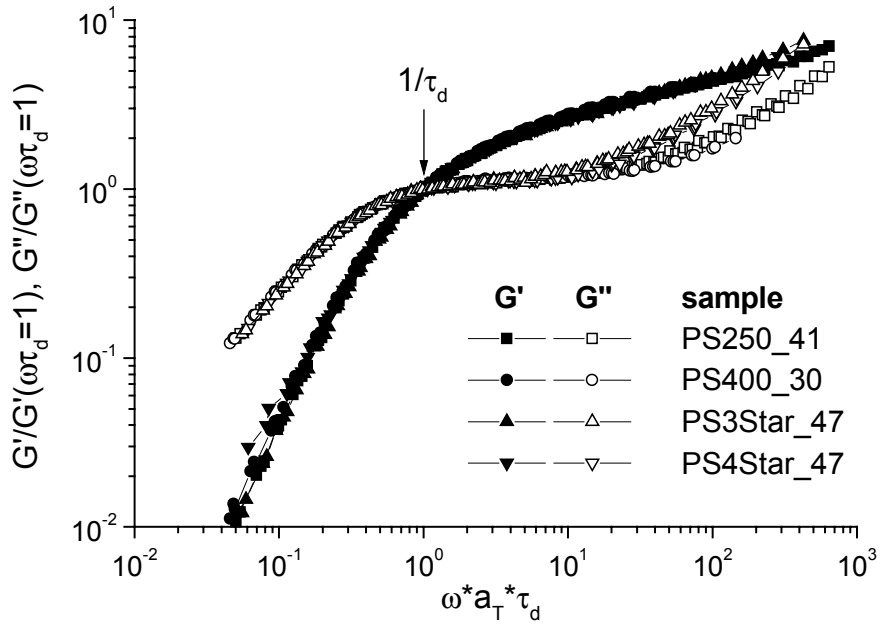
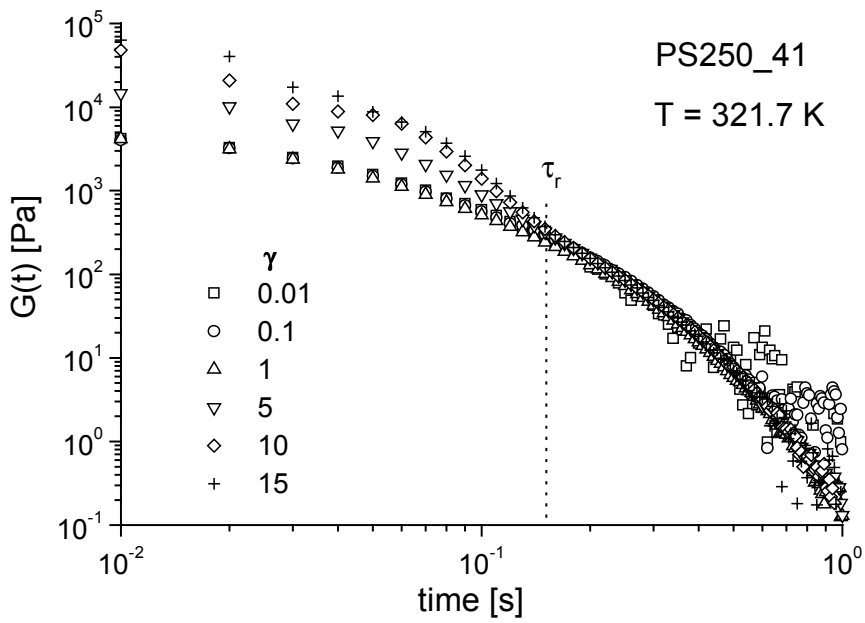


Figure 2: A



B

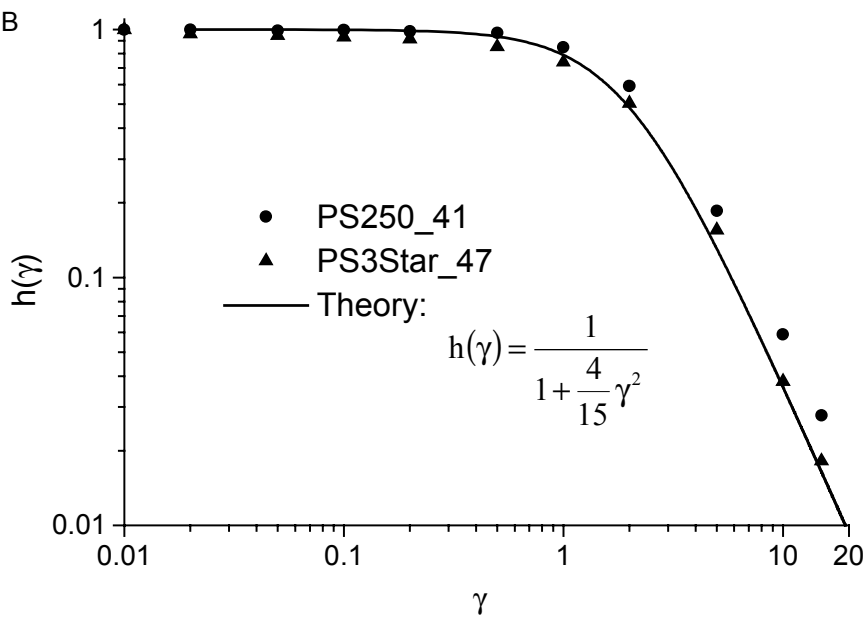
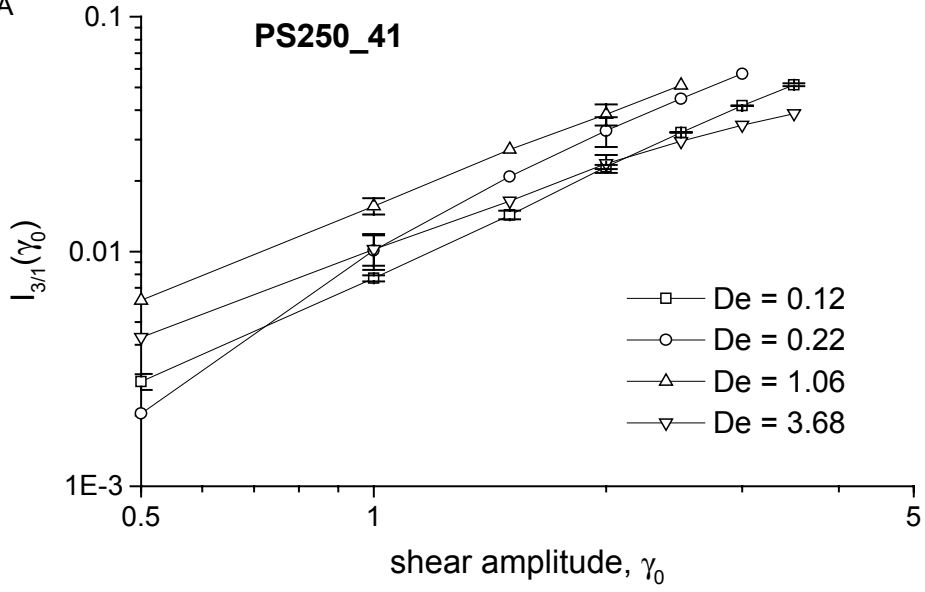


Figure 3: A



B

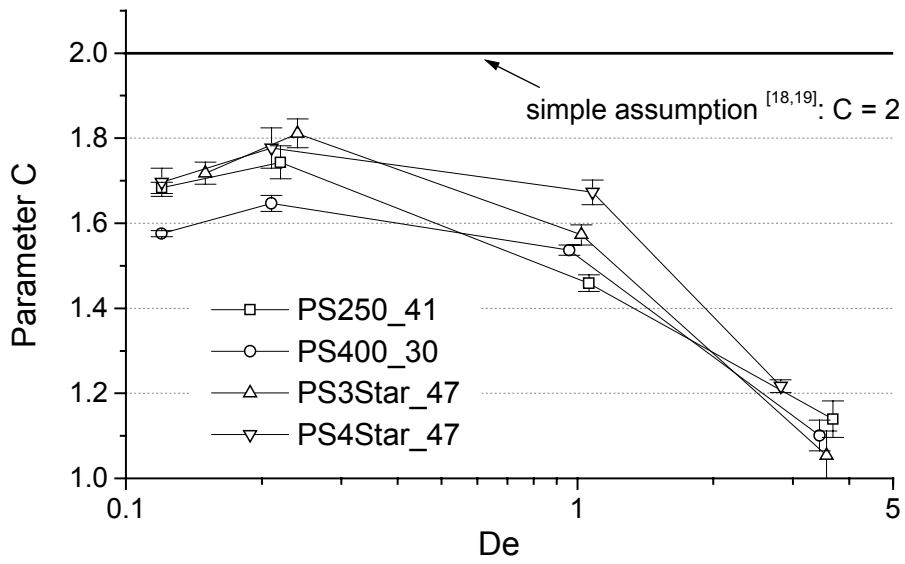


Figure 4:

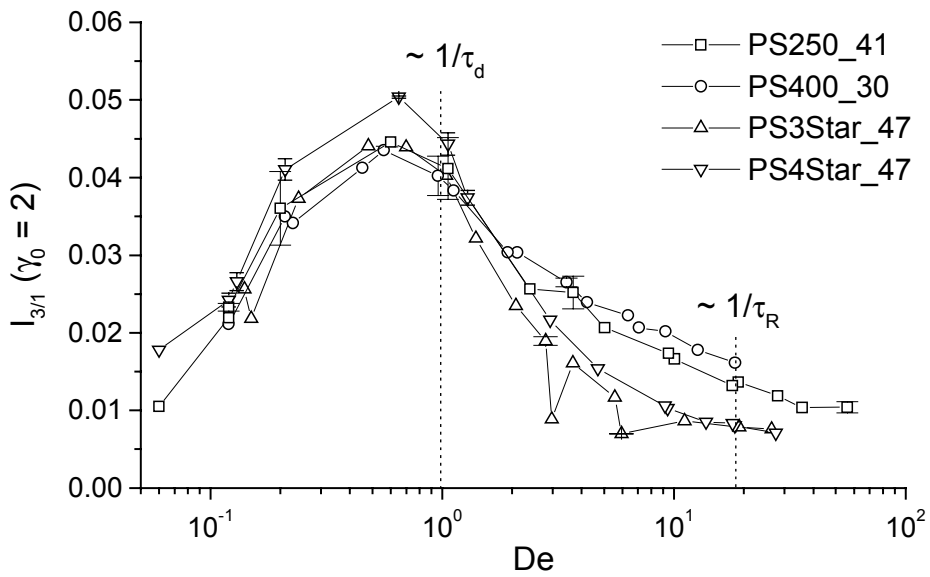


Figure 5:

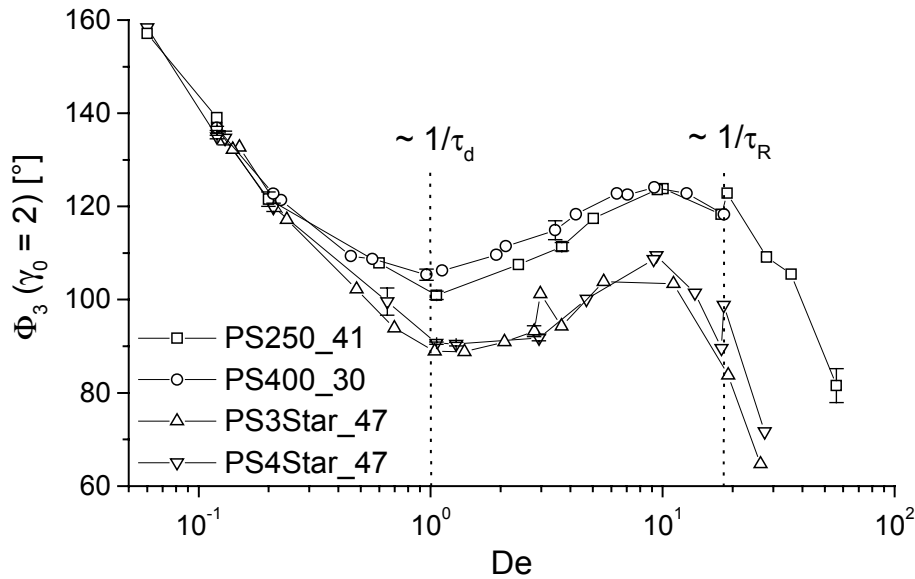


Table & Figure Caption

Table 1:

Analytical results for $I_{3/1}$, Φ_3 , and Δ_3 for several phenomenological, constitutive, and molecular models using Fourier analysis.

Table 2:

Investigated polystyrene solutions: weight-average molecular weight M_w in kg/mole and polydispersity M_w / M_n as measured by GPC, c the polymer weight fraction in the solutions, effective entanglement molecular weight M_e^{sol} in kg/mole and effective number of entanglements in the solution Z^{sol} based on the solvent mediated dilution of entanglements ^[25].

Figure 1:

Linear viscoelastic data for two linear PS solutions (PS250_41, PS400_30) and two star-shaped PS solutions (PS3Star_47, PS4Star_47). All samples are referenced to the crossover point of G' and G'' .

Figure 2:

(A) Linear viscoelastic relaxation modulus $G(t)$ as a function of time for PS250_41 at $T = 321.7$ K obtained by superimposing stress relaxation curves $G(t, \gamma)$ measured at various strain amplitudes by an amount $1/h(\gamma)$. (B) Damping functions $h(\gamma)$ for PS250_41 and PS3Star_47 in single-step shearing fitted by a simple expression following the predictions of Doi and Edwards ^[35].

Figure 3:

(A) Magnitude ratio, $I_{3/1}$, as a function of the strain amplitude, γ_0 , for PS250_41 measured at different Deborah numbers. (B) Scaling exponent C as a function of the Deborah number, De , for the polystyrene solutions. The different curves pictured in (A) were fitted using Equation 1 and the scaling exponent C was extracted.

Figure 4:

Magnitude $I_{3/1}$ as a function of the Deborah number, De , at $\gamma_0 = 2$ for polystyrene solutions with different topology.

Figure 5:

Phase difference Φ_3 as a function of the Deborah number De at $\gamma_0 = 2$ for the polystyrene solutions.

References

- [1] S. Onogi, T. Masuda, K. Kitagawa, *Macromolecules* **1970**, *3*, 109.
- [2] J.S. Dodge, I.M. Krieger, *Trans. Soc. Rheol.* **1971**, *15*, 589.
- [3] I.M. Krieger, T.F. Niu, *Rheol. Acta* **1973**, *12*, 567.
- [4] T. Matsumoto, Y. Segawa, Y. Warashina, S. Onogi, *Trans. Soc. Rheol.* **1973**, *17*, 47.
- [5] W.M. Davis, C.W. Macosko, *J. Rheol.* **1978**, *22*, 53.
- [6] D.S. Pearson, W.E. Rochefort, *J. Poly. Sci.* **1982**, *20*, 83.
- [7] A.J. Giacomin, J.M. Dealy, "Large-amplitude oscillatory shear", in: *Rheological Measurements*, A.A. Collyer, D.W. Clegg, Eds., Chapman and Hall, London 1998.
- [8] M.J. Reimers, M. Dealy, *J. Rheol.* **1996**, *40*, 167.
- [9] M.J. Reimers, M. Dealy, *J. Rheol.* **1998**, *42*, 527.
- [10] S. Tariq, A.J. Giacomin, S. Gunasekarab, *Biorheol.* **1998**, *35*, 171.
- [11] M. Wilhelm, D. Maring, H.W. Spiess, *Rheol. Acta* **1998**, *37*, 399.
- [12] M. Wilhelm, P. Reinheimer, M. Ortseifer, T. Neidhöfer, H.W. Spiess, *Rheol. Acta* **2000**, *39*, 241.
- [13] M. Wilhelm, *Macromol. Mater. Eng.* **2002**, *287*, 83.
- [14] T. Neidhöfer, M. Wilhelm, H.W. Spiess, *Appl. Rheol.* **2001**, *11*, 126.
- [15] M. Wilhelm, P. Reinheimer, M. Ortseifer, H.W. Spiess, *Rheol. Acta* **1999**, *38*, 349.
- [16] D. van Dusschoten, M. Wilhelm, *Rheol. Acta* **2001**, *40*, 395.
- [17] T. Neidhöfer, B. Debbaut, M. Wilhelm, *J. Rheol.* **2003**, *47*, 1351.
- [18] E. Helfand, D. S. Pearson, *J. Polym. Sci., Polym. Phys.* **1982**, *20*, 1249.
- [19] D.S. Pearson, W.E. Rochefort, *J. Poly. Sci.* **1982**, *20*, 83.
- [20] H.G. Elias, "An Introduction to Polymer Science", Wiley-VCH, New York 1997.
- [21] P.J. Flory, "Principles of Polymer Chemistry", Cornell University Press, Ithaca, New York 1979.
- [22] R.N. Young, R.P. Quirk, L.J. Fetters, "Anionic Polymerizations of Non-Polar Monomers Involving Lithium", in: *Adv. Poly. Sci.*, Vol. 56, Springer-Verlag, New York 1984, p. 1 ff.
- [23] L.J. Fetters, D.J. Lohse, D. Richter, T.A. Witten, A. Zirkel, *Macromolecules* **1994**, *27*, 4639.
- [24] N. Hadjichristidis, *J. Polym. Sci. Polym. Chem.* **1999**, *37*, 857.
- [25] R.H. Colby, M. Rubinstein, *Macromolecules* **1990**, *23*, 2753.
- [26] G.C. Berry, *J. Chem. Phys.* **1967**, *46*, 1338.
- [27] K. Osaki, M. Kurata, *Macromolecules* **1980**, *15*, 671.
- [28] C.M. Vrentas, W.W. Graessley, *J.Rheol.* **1982**, *26*, 359.
- [29] D.C. Venerus, C.M. Vrentas, J.S. Vrentas, *J.Rheol.* **1990**, *34*, 657.
- [30] M.H. Wagner, S.E. Stephenson, *J. Rheol.* **1979**, *23*, 489.
- [31] M. Doi, S.F. Edwards, *J. Chem. Soc. Faraday Trans. II* **1978**, *74*, 1789.
- [32] M. Doi, S.F. Edwards, *J. Chem. Soc. Faraday Trans. II* **1978**, *74*, 1802.
- [33] M. Doi, S.F. Edwards, *J. Chem. Soc. Faraday Trans. II* **1978**, *74*, 1818.
- [34] M. Doi, S.F. Edwards, *J. Chem. Soc. Faraday Trans. II* **1979**, *75*, 38.
- [35] M. Doi, S.F. Edwards, "The theory of polymer dynamics, Volume 73", 2nd Edition, Clarendon Press, Oxford 1986.
- [36] K. Osaki, K. Nishizawa, M. Kurata, *Macromolecules* **1982**, *15*, 1068.
- [37] K. Osaki, E. Takatori, M. Kurata, H. Watanabe, H. Yoshida, T. Kotaka, *Macromolecules* **1990**, *23*, 4392.
- [38] D.S. Pearson, E. Helfand, *Faraday Symp. Chem. Soc.* **1983**, *18*, 189.
- [39] C.W. Macosko, "Rheology: Principles, Measurements, and Applications", Wiley-VCH, New York 1994.
- [40] R.G. Larson, "The Structure and Rheology of Complex Fluids", Oxford University Press, New York 1999.
- [41] D.S. Pearson, A.D. Kiss, L.J. Fetters, M. Doi, *J.Rheol.* **1989**, *33*, 517.
- [42] D.S. Pearson, E. Herbolzheimer, N. Grizzuti, G. Marrucci, *J. Poly. Sci. Poly. Phys.* **1991**, *29*, 1589.
- [43] G. Marrucci, *J. Non-Newt. Fluid Mech.* **1996**, *62*, 279.
- [44] G. Ianniruberto, G. Marrucci, *J. Non-Newt. Fluid Mech.* **1996**, *65*, 241.
- [45] D.W. Mead, R.G. Larson and M. Doi, *Macromolecules* **1998**, *31*, 7895.
- [46] T.C.B. McLeish, R.G. Larson, *J. Rheol.* **1998**, *42*, 81.